arXiv:1604.08170v1 [astro-ph.SR] 27 Apr 2016

Kea: a new tool to obtain stellar parameters from low to moderate signal/noise and high-resolution Echelle spectra. [1]

Michael Endl & William D. Cochran

McDonald Observatory and Department of Astronomy, The University of Texas at Austin, Austin, TX 78712, USA

ABSTRACT

In this paper we describe *Kea* a new spectroscopic fitting method to derive stellar parameters from moderate to low signal/noise, high-resolution spectra. We developed this new tool to analyze the massive data set of the *Kepler* mission reconnaissance spectra that we have obtained at McDonald Observatory. We use *Kea* to determine effective temperatures ($T_{\rm eff}$), metallicity ([Fe/H]), surface gravity (log g) and projected rotational velocity ($v \sin i$). *Kea* compares the observations to a large library of synthetic spectra that covers a wide range of different $T_{\rm eff}$, [Fe/H] and log g values. We calibrated *Kea* on observations of well-characterized standard stars (the *Kepler* field "platinum" sample) which range in $T_{\rm eff}$ from 5000 to 6500 K, in [Fe/H] from -0.5 to +0.4 dex and in log g from 3.2 to 4.6 dex. We then compared the *Kea* results from reconnaissance spectra of 45 KOIs (Kepler Object of Interest) to stellar parameters derived from higher signal/noise spectra obtained with Keck/HIRES. We find typical uncertainties of 100 K in $T_{\rm eff}$, 0.12 dex in [Fe/H] and 0.18 dex in log g.

Subject headings: Data Analysis and Techniques — Extrasolar Planets — Stars

1. Introduction

An important step in the Follow-up Observing Program of NASA's *Kepler* mission (Borucki et al. 2010) is the acquisition of reconnaissance spectra of Kepler Objects of Interest (KOI), i.e. stars hosting transiting planet candidates. These spectra allow a more detailed characterization of the potential planet-hosting star. For most KOIs only photometrically derived properties from the Kepler Input Catalog (KIC) are known prior to reconnaissance

[1] Named after *Nestor notabilis* an alpine parrot native to New Zealand

spectroscopy. KIC uncertainities for dwarf stars between 4500 and 6500 K are $\approx$ 200 K and 0.4 dex in log g and somewhat larger for more evolved stars (Brown et al. 2011).

Stellar radii are often estimated by comparing a star's effective temperature and surface gravity to evolutionary tracks. However, the KIC does not offer tight constraints on log g (0.4 dex at best). Spectroscopic surface gravity values are often more precise and can yield tighter constraints on stellar radii. This in turn impacts the planetary radius derived from the modeling of the transit feature in the *Kepler* light curve.

A large number of different tools have been developed in order to determine fundamental stellar parameters from observed spectra. The success of these tools depends strongly on the nature of the spectra. Some techniques work best on high signal/noise (S/N) data and break down for noisy data. Others work well on high resolution spectra, but fail when line-blending becomes significant in low-resolution data. Thus, one must carefully match the technique to the type of spectra that will be obtained.

One class of techniques starts with a model stellar atmosphere and computes the emergent spectrum, given the atomic (or molecular) parameters (wavelength, excitation potential, $\log gf$, damping constants, etc.) of the spectral features. The current "gold-standard" in model atmosphere analysis of stellar spectra are self-consistent 3-D radiation-hydrodynamics simulations (e.g. Stein & Nordlund 1998, Asplund et al. 2000, Magic et al. 2013). These models succeed quite well in reproducing the details of stellar line profile shapes. However, this level of detail really demands spectra of comparable quality, with very high spectral resolution and S/N. A widely used "workhorse" alternative is the MOOG stellar atmospheric analysis code (Sneden 1973). MOOG performs a variety of spectral line analysis and spectrum synthesis tasks under the assumption of local thermodynamic equilibrium (LTE) in a 1-D stellar atmospheric model. With MOOG, one can either measure equivalent widths of individual stellar atmospheric lines of interest and compare those with model widths, or one can synthesize regions of stellar spectra for comparison with the observed spectrum. A third alternative is "Spectroscopy Made Easy", or SME (Valenti & Piskunov 1996), which also synthesizes a stellar spectrum under the assumption of LTE in a 1-D stellar atmospheric model. One can then optimize the stellar model parameters ($T_{\rm eff}$, log g and [Fe/H]) by minimizing the χ^2 difference between the observed and the synthesized SME spectra. This can be a very effective and efficient method for deriving uniform and self-consistent stellar parameters for large samples of spectra (e.g. Valenti & Fischer 2005). All three of these techniques work best on spectra of relatively high S/N and high spectral resolution.

The analysis of lower S/N spectra requires special approaches in order to achieve useful and self-consistent results. When the spectra are sufficiently noisy that individual stellar absorption lines can not be measured reliably, then one must adopt a technique that will treat

large sections of the spectrum together. The most successful of these methods involve some form of spectral matching, where the observed spectrum is compared to a library of spectra, and a comparison algorithm determines the "best" match to the observations. In some cases, the library is a set of observed spectra with carefully and self-consistently determined stellar properties, as in the `SpecMatch` code used by Petigura, Marcy, & Howard (2013). For this to work well, the library of observed spectra must be obtained with the same instrument as the target spectrum, they must all be of high signal/noise, and they need to cover the parameter space of $T_{\rm eff}$, log g and [Fe/H] rather uniformly. A viable alternative to this technique is use a library of synthetic model spectra, rather than observed spectra. This ensures that the relevant ranges of parameter space are well covered, and that all of the library spectra are completely self-consistent and noise-free. However, one must model the spectrograph instrumental function in order to compare an observed spectrum with the library spectra. This approach of synthetic spectra has been used by Buchhave et al. (2012) to perform a uniform analysis of relatively low signal/noise spectra from different spectrographs. A new version of `SpecMatch` now uses a grid of synthetic models (Petigura et al. 2015, in preparation).

In this paper, we present *Kea*, a code that we developed at McDonald Observatory to compare high-resolution, low S/N spectra of KOI stars to a massive grid of synthetic stellar spectral models in order to determine the fundamental stellar parameters of the *Kepler* target stars. Our paper is organized as follows: section 2 describes the our spectroscopic observations and data reduction. In Section 3, we detail how we created a grid of synthetic spectra using the MOOG spectrum synthesizer. In Section 4, we describes the calibration of *Kea* using 100 well-characterized stars from the *Kepler* stellar properties catalog (Huber et al. 2014, = H14 hereafter), the so-called "platinum" star sample. Finally, in Section 5 we present a comparison of *Kea* results from our McDonald Observatory reconnaissance spectra with stellar parameters derived from higher S/N Keck/HIRES spectra of the same KOI.

2. Reconnaissance Spectroscopy & Data Reduction

We use the Tull Coudé Spectrograph (Tull et al. 1995) at the Harlan J. Smith 2.7 m Telescope at McDonald Observatory to obtain the reconnaissance spectra. We observe with a 1.2-arcsecond slit, which yields a spectral resolving power of $R = \lambda/\delta\lambda = 60,000$. The complete visual spectrum (3750 – 10200 Å) is imaged on a 2k×2k CCD detector.

After flat-fielding, bias-subtraction and order extraction, using standard IRAF routines, we divide each order by the appropriate blaze-function. We determine the shape for the blaze-function for each night using high-S/N flat field lamp exposures. This division removes the

large-scale curvature due to the blaze. We then apply an additional correction to each order to remove any residual curvature in the continuum.

The uncertainty of each pixel $\sigma_{\rm pixel}$ in the extracted spectrum is calculated as:

$$\sigma_{\rm pixel} = \sqrt{N_{\rm pixel} + n\sigma^2_{\rm readout}} \quad (1)$$

Where $N_{\rm pixel}$ are the total number of detected photo-electrons in a pixel, n is the number of pixels in a column that were combined during order extraction, and $\sigma_{\rm readout}$ is the readout noise. For the Tull spectra we use $n = 5$ and $\sigma_{\rm readout} = 3.06$ electrons.

Finally, we flux-normalize the spectral orders to unity, scaling the pixel uncertainties accordingly. Figure 1 shows an example of one order of a typical KOI reconnaissance spectrum before and after these preparatory steps.

3. Synthetic Spectral Library

We computed a large grid of model stellar spectra using the 'synth' mode of the LTE stellar spectral line analysis and spectrum synthesis MOOG. We used the Kurucz (1993) stellar atmosphere grid, with the "ODFNEW" opacity distribution function. Spectra were synthesized from 3450 Å to 7000 Å. The complete spectral grid covers a range of $T_{\rm eff}$ from 3500 K to 7000 K in 100 K steps, and from 7000 K to 10,000 K in steps of 200 K. We used [Fe/H] to represent overal stellar metallicity. Model spectra were computed with [Fe/H] ranging from -1.0 to +0.5 dex in 0.25 dex steps. All models used a solar value of [α/Fe]. Stellar surface gravity was varied from 1.0 to 4.0 in steps of 0.5 dex and from 4.0 to 5.0 in steps of 0.25 dex. No spectra were computed with $\log g = 1.50$ for $T_{\rm eff}$ from 9200 K to 10,000 K nor for $\log g = 1.00$ for $T_{\rm eff}$ from 8400 K to 10,000 K as those regions of parameter space were not covered by the Kurucz (1993) model atmospheres. The final grid comprises a total of 8752 synthetic spectra.

We obtained atomic line parameters ($\log gf$, excitation potential, and damping parameters) from VALD (Vienna Atomic Line Database, Kupka et al. 2000). We included molecular opacities for MgH (Bernath et al. 1985, Hinkle et al. 2013), TiO (Plez, 1998), and CN (Sneden et al. 2014). The MgH line list included ^{24}MgH lines in the A $^2\Pi$-X $^2\Sigma^+$ system listed by Bernath et al. (1985), supplemented by ^{25}MgH and ^{26}MgH lines from the compillation of Hinkle et al. (2013). For CN, we limited our consideration to ^{12}C^{14}N lines in the A $^2\Pi$-X $^2\Sigma^+$ (red) and B $^2\Sigma^+$-X $^2\Sigma^+$ (violet) systems. Both of these linelists are available from the

MOOG labdata web page[2]. The TiO line list included only the $^{48}Ti^{16}O$ isotopologue. In all, our final line list included approximately 3.3 million spectral lines. For each synthetic spectrum calculation, we employed the MOOG "weedout" feature to remove atomic and molecular lines from the linelist with a ratio of line to continuum opacity of less than 0.001. A separate line list of "strong" spectral lines was used so that the extended damping wings of H Balmer lines, and certain lines of Na, Mg, Ca, Cr, Mn and Fe could be computed fully.

4. Fitting the Data

Before *Kea* can match the synthetic spectra to the observed spectral orders, the synthetic spectra need to be convolved with the appropriate point-spread-function (PSF) to assure the same spectral resolution of model and data. For this purpose, we convolve the synthetic spectrum with a Gaussian-shaped PSF and down-sample the model to set it on the same pixel scale as the observation. For each order we calculate the correct width of the PSF for an $R = 60,000$ spectrum with 2048 model pixels. In addition to this PSF-convolution, *Kea* also applies a standard rotational broadening function for stellar lines as derived in Gray (2005). The rotational broadening will likely also absorb any residual PSF broadening for spectra where the resolution is slightly different to $R = 60,000$. We did not include macroturbulence as a line broadening effect. We think that the inclusion of macroturbulence as an additional model parameter is not warranted, given the typically moderate to low S/N values of the spectra that *Kea* is applied to. The rotational broadening will likely absorb any macroturbulence effects and might therefore be slightly overestimated. After these steps, the model spectrum is ready to be compared to the data. *Kea* is using the standard χ^2 criterion for the goodness-of-fit test.

In the next step we determine the wavelength shift $\delta\lambda$ between the model and the observation. This $\delta\lambda$ is caused by the combination of the absolute radial velocity of the target star and the Earth's motion at the time of observation. For this purpose we use one spectral order and shift a default model with no rotational broadening and solar $T_{\rm eff}$, [Fe/H] and log g until a χ^2-minimum is found that corresponds to the $\delta\lambda$ between model and data. We apply the $\delta\lambda$ that corresponds to the χ^2-minimum to all *Kea* model orders for this particular spectrum. In some cases, particularly for very low S/N data, one order is not enough to determine the $\delta\lambda$ shift. Under these circumstances we typically use 4 to 5 different spectral orders to find the correct $\delta\lambda$.

To save computational time, *Kea* does not compare the entire grid of synthetic spectra

[2]http://www.as.utexas.edu/∼chris/lab.html

to every single observed spectral order. We adopted a two-step approach:

1. *Kea* is run using a coarse step size in all four parameters spanning the entire range of the synthetic grid. From 3500 K to 7000 K $T_{\rm eff}$ we use a step of 500 K in $T_{\rm eff}$ and from 7000 K to 10,000 K a step of 1000 K, for [Fe/H] we use the four values of -1.0,-0.5,0.0, and +0.5, and for log g we use the values 1.0, 2.0, 3.0, 4.0, 4.5,and 5.0. For $v \sin i$ in the range from 1 to $15\,{\rm km\,s^{-1}}$ we move in steps of $2\,{\rm km\,s^{-1}}$ and then from 20 to $60\,{\rm km\,s^{-1}}$ in steps of $10\,{\rm km\,s^{-1}}$. For each spectral order, *Kea* determines the χ^2-value and records the best-fit model for each order. The final parameters and uncertainties that *Kea* reports for a spectrum are the mean values of the model parameters of all best-fit models and the formal uncertainty of this mean (=RMS/$\sqrt{N}$ with N the number of orders used to determine the mean). This initial run yields a first "guess" set of stellar parameters that we use as input parameters for step 2. In case of a fast rotator with $v \sin i > 60\,{\rm km\,s^{-1}}$ the best-fit models for all orders will have the maximum value of $60\,{\rm km\,s^{-1}}$. For these targets we expand the range of trial $v \sin i$ values even further.

2. in the second step, we run *Kea* using the densest possible step size that is set by the model grid itself: $T_{\rm eff}$ in 100 K, [Fe/H] and log g in 0.25 dex steps, and $v \sin i$ in $1\,{\rm km\,s^{-1}}$ steps (except for fast rotators where we use steps of 5-10 $\rm km\,s^{-1}$). In contrast to the previous step we now limit the range that *Kea* searches in the model grid to $T_{\rm eff}$ values that are ±500 K, ±1.5dex in log g and $\pm 5\,{\rm km\,s^{-1}}$ in $v \sin i$ from the first-guess values from step 1 using the whole range of [Fe/H] values in our library. As before, we record the best-fit (χ^2-minimum) models for each spectral order that *Kea* analyzes and determine the final stellar parameters from the mean and scatter of these values.

Figure 2 shows 12 spectral orders from one observed KOI spectrum (blue) and the corresponding best-fit *Kea* model in green and the residuals in red.

5. Calibration with Platinum star sample

To test *Kea* we used the so-called "platinum" star sample of the *Kepler* follow-up observing program. The platinum stars are a carefully selected group of stars from the *Kepler* stellar properties catalog (H14) that all have asteroseismically derived log g values with very small uncertainties of the order of 0.03 dex. During the 2014 *Kepler* observing season we collected spectra for 100 platinum stars, using the exact same instrumental setup as for the KOI observations. The stars range in $T_{\rm eff}$ from 5000 to 6700 K, in [Fe/H] from -1.0 to +0.5 and in log g from 3.3 to 4.6 dex. The majority of the sample are slow rotators with only 12 stars having a $v \sin i > 10\,{\rm km\,s^{-1}}$. Out of these 12 only 5 stars have $v \sin i > 30\,{\rm km\,s^{-1}}$.

A detailed description of the selection criteria of the platinum sample and a comparison of different methods to derive stellar parameters will be presented in a future publication (Furlan et al. 2016, in prep.)

The platinum stars are also significantly brighter than the KOIs we observe at McDonald Observatory, which reflects in a much higher S/N for the platinum star spectra. Typically, a KOI reconnaissance spectrum has a S/N of 20-30 per resolution element at 5650 Å, while the platinum star spectra have S/N$\approx$ 80.

We used *Kea* to derive stellar parameters from these 100 spectra. We compared the overall mean offset and RMS-scatter of the 100 *Kea* values with the published values for each of the 21 orders of the Tull spectrum that covers the wavelength range of our library. Table 1 contains the complete information of this order by order comparison and the result is displayed in Figure 3. We calibrateb *Kea* by testing which spectral orders yield the smallest offsets from, and smallest scatter around, the reported values in H14. With this procedure we identify spectral orders that are sensitive to the stellar parameter that we want to determine. We achieved best results by using 13 (out of these 21) spectral orders which satisfy the following criteria: the mean offset in $T_{\rm eff}$ is less than 110 K and the overall scatter of the values is less than 200K, the offset in [Fe/H] is less then 0.1 dex and the RMS is less than 0.2 dex, and for log g we selected orders that have an offset of less than 0.1 dex and an RMS less than 0.3 dex. The resulting selection of orders are displayed in Figure 3 with a (green) shaded background. All 13 orders are being used to measure the $v \sin i$.

For $T_{\rm eff}$ and [Fe/H] we can perform this calibration only for a subset of 63 stars that also have spectroscopically derived [Fe/H] and $T_{\rm eff}$ listed in H14 (the remaining 36 stars have these values estimated from photometry and [Fe/H] set to a default value of -0.2 ± 0.3). The uncertainties in $T_{\rm eff}$ for these 63 stars is 119 ± 8 K. The uncertainties for the spectroscopically derived [Fe/H] values in H14 are given as 0.15 dex. Our calibration yield in effective temperature a small offset of -25 K with an RMS-scatter of 89 K. For the metallicity we achieved an offset of -0.02 dex and an RMS of 0.07 dex. For surface gravity we can use all 100 stars and compare it to the asteroseismically derived log g values. The *Kea* results show a small offset of -0.0006 dex, smaller than the H14 uncertainties, and an RMS-scatter of 0.11 dex.

In Figure 4 we display the dependence of the difference between the *Kea* results and the values from H14 on the value of this parameter. We do not see any strong systematic trends in these differences.

6. Comparison with Keck/HIRES SME results

After the calibration with the high S/N platinum star spectra, we tested *Kea* on data in the S/N range that is typical for our *Kepler* mission reconnaissance observations. We compared the *Kea* results for 45 reconnaissance spectra of 32 KOIs from the beginning of the mission (all with KOI numbers < 1000) with the results derived from Keck/HIRES spectra. The Keck data were analyzed with SME and we took the stellar parameters that are posted in the notes section of each KOI on the CFOP webpage[3]. In a few cases, we took the stellar parameters from the published literature: e.g. KOI-87: Borucki et al. (2012); KOI-128: Endl et al. (2012); KOI-135, KOI-183 and KOI-214: Endl et al. (2014). The S/N of the 45 Tull reconnaissance spectra at 5650 Å ranges from 13 to 133 per resolution element, with a mean of 28 and a standard deviation of 19. The effective temperature range of these data is 4700 to 6100 K, in [Fe/H] from -0.55 to +0.45 and in log g from 3.9 to 4.7 dex.

We display the results in Figure 5. In effective temperature we find an average offset of +80 K and an RMS-scatter of 100 K. The *Kea* $T_{\rm eff}$ values are systematically higher than the SME values, especially in the 5200 to 5600 K range. For the metallicity parameter we see an offset of-0.04 dex and a standard deviation of 0.12 dex. And for the surface gravity we find a very small offset of +0.002 dex with an RMS-scatter of 0.18 dex between the Keck results and ours. Table 2 lists the SME and *Kea* values from this test along with the KOI number and the S/N of the Tull spectra (we do not have access to the S/N values of the HIRES spectra).

The slightly larger offset in $T_{\rm eff}$ and the increased scatter of these results, as compared to the platinum star sample calibration, might be due to the lower S/N of the Tull spectra. We tested this hypothesis by artifically degrading the S/N of the platinum star spectra. We used a subset of 30 spectra that originally have $\Delta T_{\rm eff} = -24 \pm 110$ K, Δ[Fe/H] $= 0.02 \pm 0.09$ dex and Δ log $g = 0.0006 \pm 0.108$ dex. Degrading these spectra to S/N=30 yielded the following values: $\Delta T_{\rm eff} = 13 \pm 123$ K, Δ[Fe/H] $= 0.06 \pm 0.09$ dex and Δ log $g = 0.04 \pm 0.19$ dex. Decreasing the S/N further down to S/N=20 we obtained $\Delta T_{\rm eff} = 33 \pm 124$ K, Δ[Fe/H] $= 0.08 \pm 0.11$ dex and Δ log $g = 0.22 \pm 0.29$ dex. These results indicate that a major contribution to the larger offsets and RMS-scatter for the SME-*Kea* comparison is simply lower S/N.

[3]https://cfop.ipac.caltech.edu/

7. Limitations of *Kea*

Owing to the specific calibration of *Kea* we note that results for stars with effective temperatures outside the range of the platinum sample (5000 - 6700 K) might have larger uncertainties than the ones quoted here. Also, *Kea* is not tested for rapid rotators with $v \sin i > 30\,\mathrm{km\,s^{-1}}$. Finally, our results indicate that stellar parameters derived with *Kea* from spectra with S/N less than 20 are unreliable.

8. Conclusions

We present a description of the new *Kea* spectroscopic fitting tool, which we use to derive stellar parameters ($T_{\rm eff}$, [Fe/H], $\log g$ and $v \sin i$) for the *Kepler* mission reconnaissance spectra that we collect with the Tull spectrograph at the Harlan J. Smith 2.7 m telescope at McDonald Observatory. A calibration with the sample of 100 platinum stars yield typical uncertainties of ±90 K in effective temperature, of ±0.07 dex in [Fe/H] and of ±0.11 dex in $\log g$. We tested *Kea* by comparing it to stellar parameters derived from higher S/N Keck/HIRES spectra for 32 KOIs and 45 Tull spectra in the S/N range of our reconnaissance observations. We find a typical RMS-scatter of 100 K in $T_{\rm eff}$, 0.12 dex in [Fe/H], and 0.18 dex in $\log g$.

Kea is now in routine operation to obtain spectroscopically determined parameters from the KOI reconnaissance data that the McDonald Observatory *Kepler* follow-up observing team are collecting. We have used *Kea* recently to analyze spectra of Kepler-452 (Jenkins et al. 2015), a G2 star orbited by a 1.6 $R_\oplus$ planet inside its circumstellar habitable zone.

The *Kepler* Follow-Up Observing Program observations at McDonald Observatory are supported by NASA Grant NNX13AB62A from NASA Ames Research Center. ME acknowledges support by NASA under Grant NNX14AB86G issued through the Kepler Participating Scientist Program. This work has made use of the VALD database, operated at Uppsala University, the Institute of Astronomy RAS in Moscow, and the University of Vienna. We are extremely grateful to Chris Sneden and Erik Brugamyer for their patient advice and assistance in our use of MOOG, and to Phillip J. MacQueen, who helped with many important discussions during the development of *Kea*. We also thank the entire *Kepler* community follow-up observing (CFOP) working group, led by David Ciardi, who helped with coordianting the reconnaissance and platinum star observations. Funding for the Discovery mission *Kepler* is provided by NASA's Science Mission Directorate.

REFERENCES

Asplund, M.; Nordlund, Å; Trampedach, R.; Allende Prieto, C.; Stein, R. F. 2000, A&A, 359, 729

Bernath, P. F.; Black, J. H.; Brault, J. W. 1985, ApJ, 298, 375

Borucki, W. J.; et al. 2010, Science, 327, 977

Borucki, W. J.; et al. 2012, ApJ, 745, 120

Brown, T. M., Latham, D. W., Everett, M. E., & Esquerdo, G. A. 2011, AJ, 142, 112

Buchhave, L. A. et al. 2012, Nature, 486, 375

Gray, D. F. 2003, The Observation and Analysis of Stellar Photospheres, Cambridge University Press.

Endl, M.; MacQueen, P. J.; Cochran, W. D.; Brugamyer, E. J. et al. 2012, ApJS, 197, 13

Endl, M.; Caldwell, Douglas A.; Barclay, Thomas; Huber, Daniel; et al. 2014, ApJ, 795, 151

Hinkle, K. H. et al. 2013, ApJS, 207, 26

Huber, D. et al. 2014, ApJS, 211, 2

Jenkins, J. M., Twicken, J. D., Batalha, N. M., et al. 2015, AJ, 150, 56

Kupka, F. G.; Ryabchikova, T. A.; Piskunov, N. E.; Stempels, H. C.; Weiss, W. W. 2000, Baltic Astronomy, 9, 590

Kurucz, R. 1993, ATLAS9 Stellar Atmosphere Programs and 2 km/s grid, Kurucz CD-ROM No. 13 (Cambridge, MA: Smithsonian Astrophysics Observatory)

Magic, Z.; Collet, R.; Asplund, M.; Trampedach, R.; Hayek, W.; Chiavassa, A.; Stein, R. F.; Nordlund, Å 2013, A&A, 557, A26

Petigura, E. A.; Marcy, G. W.; Howard, A. W. 2013, ApJ, 2013, 770, 69

Plez, B. 1998 A&A, 337, 495

Sneden, C. A. 1973, PhD thesis, Univ. Texas at Austin

Sneden, C. A. et al. 2014, ApJS, 214, 26

Stein, R. F. and Nordlund, Å 1998, ApJ, 499, 914

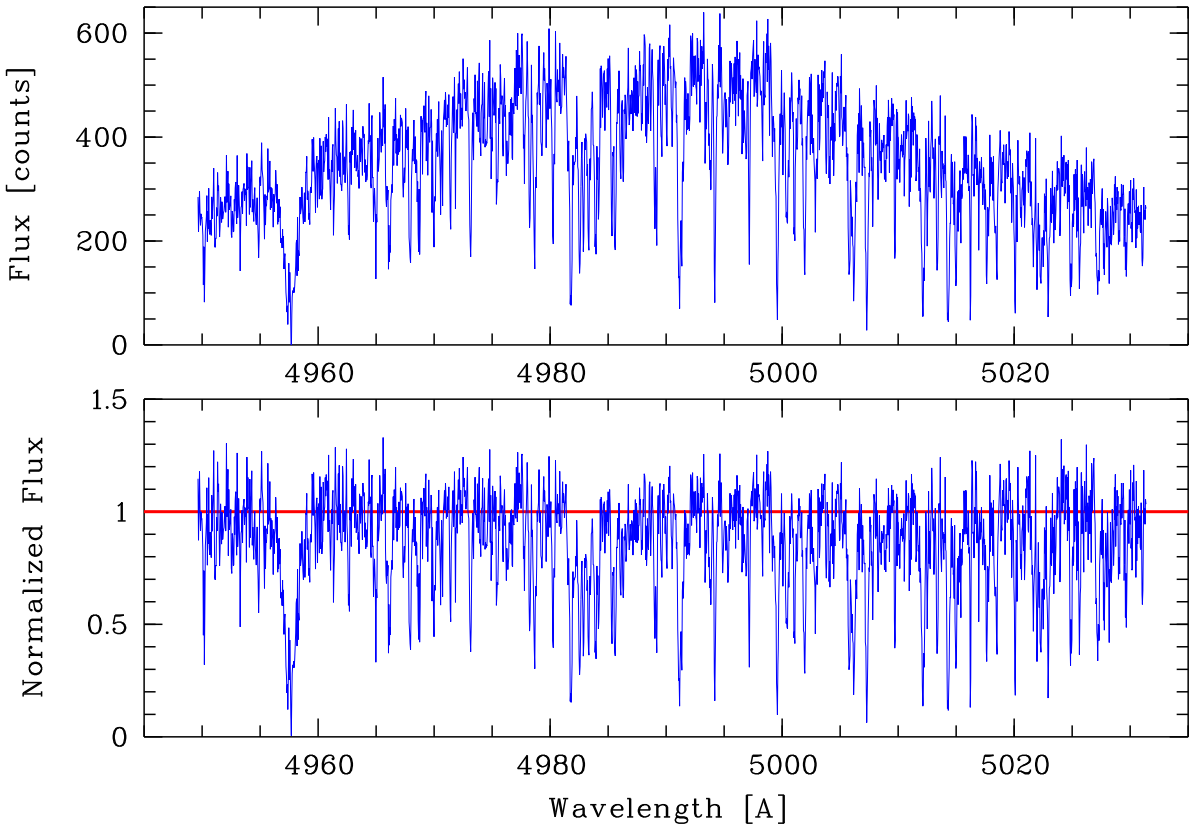

Fig. 1.— Example of a KOI reconnaissance spectrum before (top panel) blaze division and residual continuum flattening and after (bottom panel). The S/N of this spectrum at the top of the blaze of the order is S/N$\approx 17:1$.

Tull, R. G., MacQueen, P. J., Sneden, C., Lambert, D. L. 1995, PASP, 107, 251

Valenti, J. A. & Piskunov, N. 1996, A&AS, 118, 595

Valenti, J. A. & Fischer, D. A. 2005, ApJS, 159, 141

This preprint was prepared with the AAS LaTeX macros v5.2.

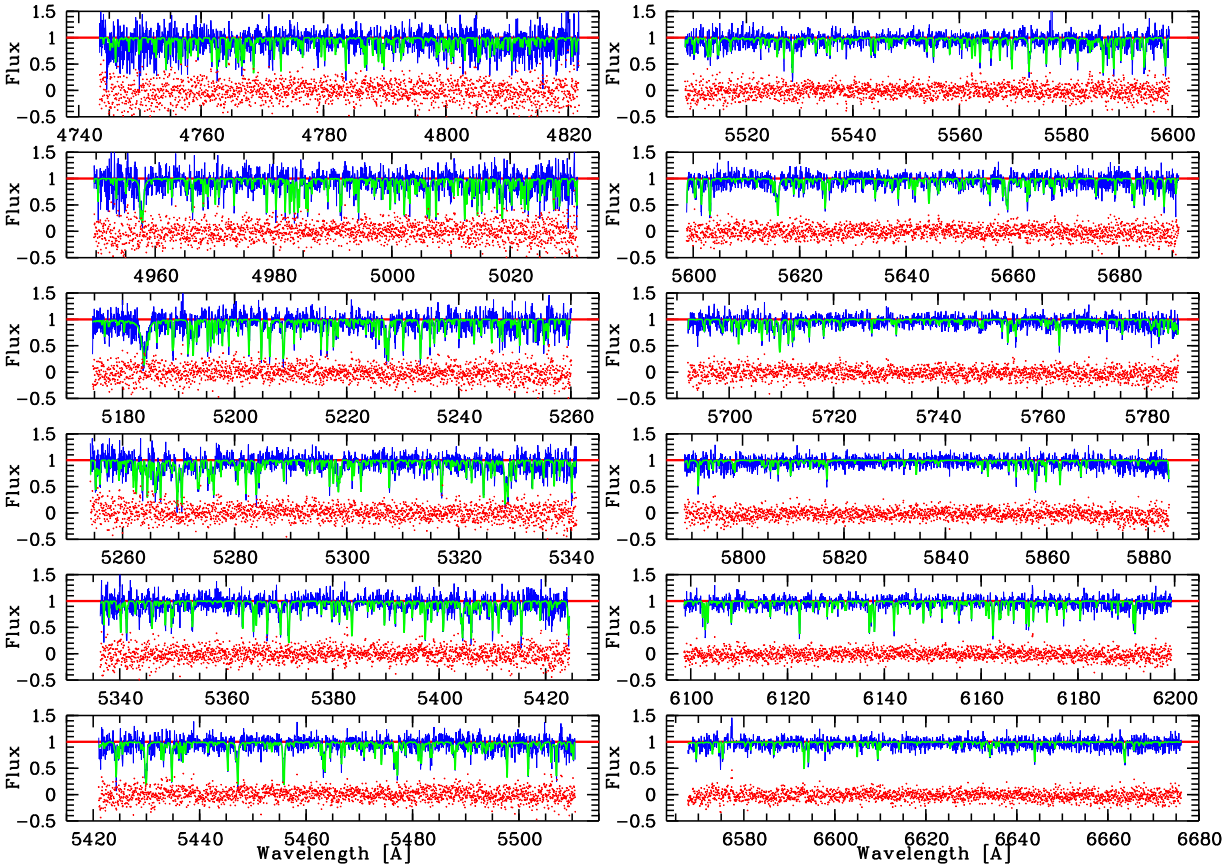

Fig. 2.— Comparison of an observed spectrum (blue) to best-fit *Kea* models in green (residuals in red) for 12 spectral orders of one typical KOI reconnaisssance spectrum with a S/N of 23 at 5650 Å.

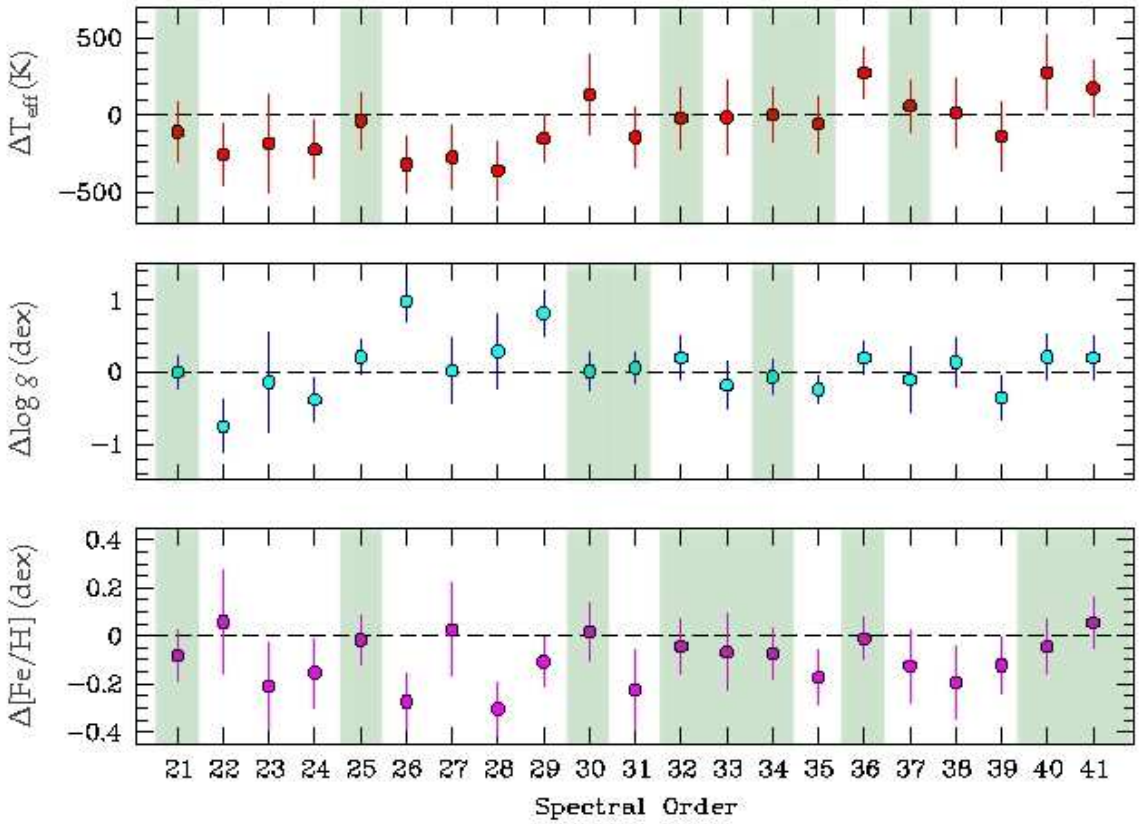

Fig. 3.— The difference between individual spectral order results from *Kea* and the published values from Huber et al. (2014). The 13 orders that are shown with a green shaded background were selected to provide information on the particular stellar parameter (see text for details on the selection criteria).

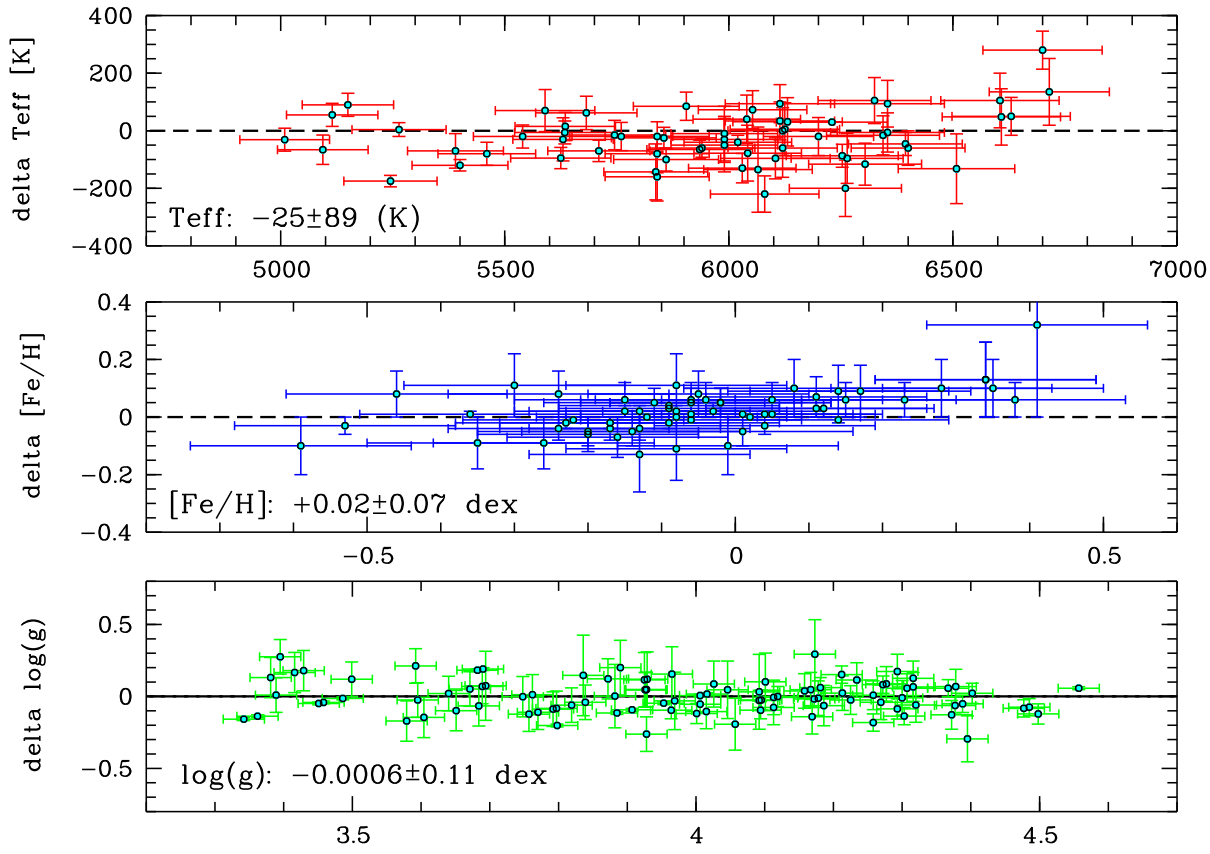

Fig. 4.— The difference between *Kea* results and the Huber et al. (2014) catalog as function of the effective temperature of the star (upper panel), metallicity (middle panel) and log g (bottom panel). There are no obvious systematic trends visible. In effective temperature we have an offset of -25 K and an RMS-scatter of 89 K. In [Fe/H] we find a mean offset of +0.02 with an RMS-scatter of 0.07 dex. In $\log g$ the respective values are -0.0006 and 0.11 dex.

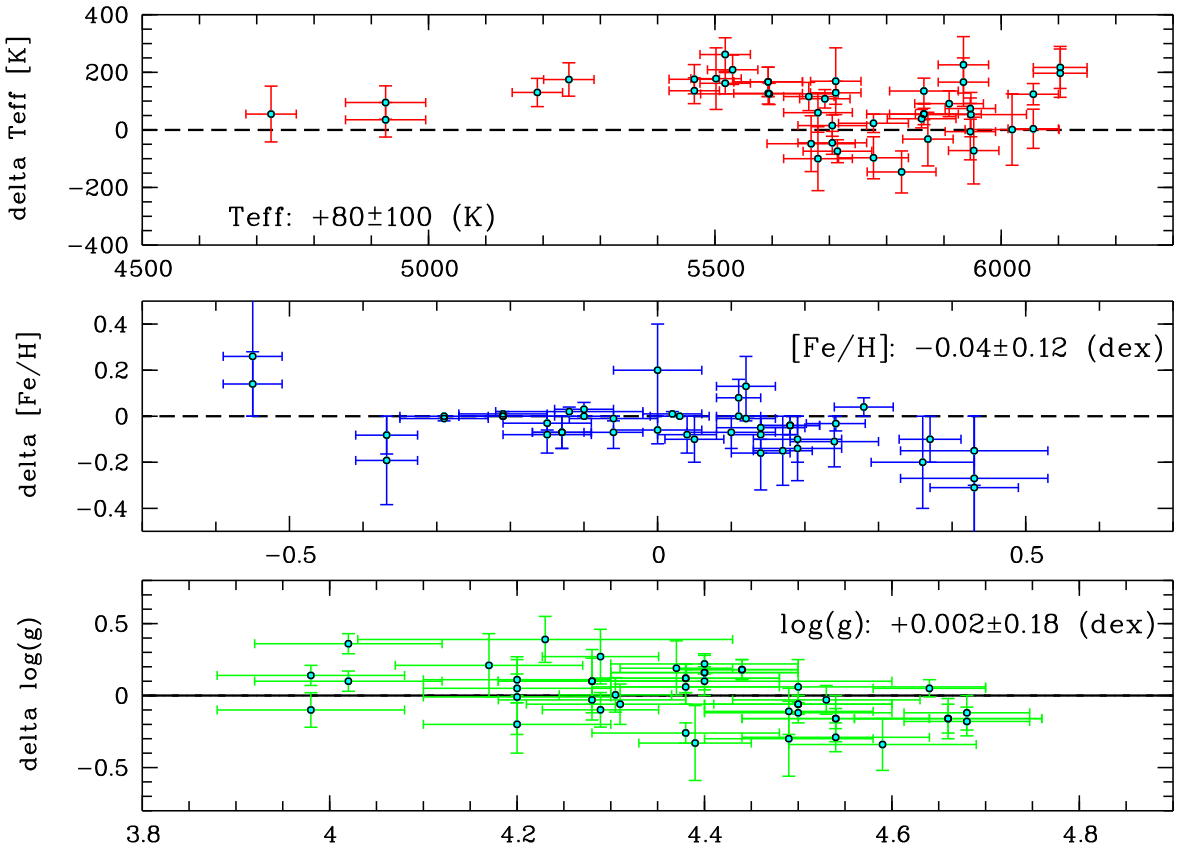

Fig. 5.— Comparison of the *Kea* results for 45 reconnaissance spectra with the parameters obtained with SME from Keck/HIRES spectra (posted on CFOP website). In $T_{\rm eff}$ we find an offset of 80 K (the Kea values are higher) and an RMS-scatter of 100 K, in [Fe/H] the offset is -0.04 with an RMS of 0.12 dex and in log g the offset is +0.002 with an RMS of 0.18 dex.

Table 1. The comparison of the *Kea* results from all Tull spectral orders with the Huber et al. (2014) values. In each column we list the average offset and RMS-scatter of the *Kea* values. A "$\star$" indicates that this order is selected to obtain information on this particular parameter (see also Figure 3).

order	λ range (Å)	$\Delta T_{\rm eff}$ (K)	Δ [Fe/H] (dex)	Δ log g (dex)
41	4740 - 4820	173.4 ± 177	$0.05 \pm 0.11\star$	0.20 ± 0.31
40	4810 - 4890	275.3 ± 242	$-0.05 \pm 0.11\star$	0.21 ± 0.31
39	4880 - 4960	-135.6 ± 223	-0.12 ± 0.12	-0.35 ± 0.31
38	4940 - 5030	14.4 ± 224	-0.19 ± 0.15	0.14 ± 0.34
37	5020 - 5110	$59.4 \pm 171\star$	-0.13 ± 0.15	-0.10 ± 0.46
36	5090 - 5180	272.4 ± 166	$-0.01 \pm 0.09\star$	0.20 ± 0.23
35	5180 - 5260	$-58.6 \pm 182\star$	-0.17 ± 0.11	-0.24 ± 0.20
34	5260 - 5340	$0.4 \pm 173\star$	$-0.07 \pm 0.10\star$	$-0.07 \pm 0.24\star$
33	5330 - 5420	-15.6 ± 243	$-0.07 \pm 0.16\star$	-0.18 ± 0.33
32	5420 - 5520	$-19.6 \pm 195\star$	$-0.04 \pm 0.11\star$	0.20 ± 0.31
31	5500 - 5600	-142.6 ± 195	-0.22 ± 0.17	$0.06 \pm 0.22\star$
30	5600 - 5690	132.4 ± 253	$0.02 \pm 0.12\star$	$0.01 \pm 0.26\star$
29	5690 - 5790	-152.6 ± 152	-0.11 ± 0.10	0.81 ± 0.31
28	5780 - 5890	-359.6 ± 187	-0.30 ± 0.11	0.29 ± 0.52
27	5890 - 5985	-275.6 ± 206	$0.03 \pm 0.19\star$	0.02 ± 0.46
26	5990 - 6090	-318.6 ± 185	-0.27 ± 0.12	0.98 ± 0.29
25	6100 - 6200	$-37.6 \pm 177\star$	$-0.02 \pm 0.10\star$	0.21 ± 0.24
24	6210 - 6315	-224.6 ± 190	-0.15 ± 0.14	-0.38 ± 0.30
23	6335 - 6430	-183.6 ± 319	-0.21 ± 0.18	-0.14 ± 0.69
22	6440 - 6550	-258.6 ± 198	0.06 ± 0.21	-0.75 ± 0.37
21	6550 - 6680	$-109.6 \pm 190\star$	$-0.08 \pm 0.105\star$	$-0.001 \pm 0.24\star$

Table 2. The comparison of the *Kea* results for 45 KOIs with the values from an SME analysis of Keck/HIRES spectra of the same object.

KOI	S/N 5650Å	$T_{\rm eff}$ SME	σ SME	[Fe/H] SME	σ SME	log g SME	σ SME	$T_{\rm eff}$ *Kea*	σ *Kea*	[Fe/H] *Kea*	σ *Kea*	log g *Kea*	σ *Kea*
005	43.8	5861.	60.	0.14	0.06	4.17	0.10	5900.	32.	0.09	0.03	4.38	0.22
007	44.3	5865.	60.	0.19	0.06	4.28	0.10	6000.	45.	0.05	0.04	4.38	0.22
007	66.5	5865.	60.	0.19	0.06	4.28	0.10	5920.	20.	0.09	0.03	4.25	0.14
017	29.0	5826.	60.	0.43	0.06	4.59	0.10	5680.	73.	0.12	0.05	4.25	0.18
041	43.3	5909.	60.	0.10	0.06	4.28	0.10	6000.	45.	0.03	0.02	4.38	0.16
069	52.0	5593.	60.	-0.21	0.06	4.50	0.10	5760.	51.	-0.21	0.02	4.44	0.06
069	53.3	5593.	60.	-0.21	0.06	4.50	0.10	5760.	51.	-0.20	0.03	4.38	0.07
069	80.3	5593.	60.	-0.21	0.06	4.50	0.10	5720.	37.	-0.21	0.02	4.44	0.06
072	48.2	5705.	60.	-0.15	0.06	4.54	0.10	5660.	40.	-0.23	0.04	4.25	0.10
072	133.0	5705.	60.	-0.15	0.06	4.54	0.10	5720.	37.	-0.18	0.02	4.38	0.07
084	53.0	5464.	44.	-0.13	0.04	4.38	0.10	5640.	51.	-0.20	0.03	4.50	0.10
084	59.3	5464.	44.	-0.13	0.04	4.38	0.10	5600.	45.	-0.20	0.02	4.50	0.10
087	55.2	5518.	44.	-0.29	0.06	4.44	0.06	5680.	37.	-0.30	0.03	4.62	0.07
087	59.4	5518.	44.	-0.29	0.06	4.44	0.06	5780.	58.	-0.29	0.02	4.62	0.07
097	30.4	5934.	44.	0.11	0.03	3.98	0.10	6160.	98.	0.19	0.03	3.88	0.12
097	45.8	5934.	44.	0.11	0.03	3.98	0.10	6100.	84.	0.11	0.02	4.12	0.07
103	30.3	5531.	44.	-0.06	0.04	4.40	0.10	5740.	51.	-0.13	0.03	4.62	0.07
108	28.0	5946.	44.	0.14	0.04	4.20	0.10	5940.	98.	0.06	0.04	4.25	0.10
108	49.5	5946.	44.	0.14	0.04	4.20	0.10	6020.	37.	-0.02	0.04	4.31	0.16
111	23.6	5711.	44.	-0.55	0.04	4.20	0.10	5880.	116.	-0.29	0.06	4.19	0.26
111	27.0	5711.	44.	-0.55	0.04	4.20	0.10	5840.	40.	-0.41	0.03	4.00	0.20
116	39.6	5865.	100.	-0.12	0.10	4.40	0.20	5920.	37.	-0.10	0.04	4.50	0.10
122	37.6	5714.	60.	0.24	0.06	4.38	0.10	5640.	40.	0.13	0.03	4.12	0.07
123	37.9	5947.	97.	-0.06	0.06	4.31	0.10	6000.	77.	-0.07	0.04	4.25	0.14
127	27.7	5668.	77.	0.43	0.10	4.53	0.10	5620.	97.	0.16	0.03	4.50	0.10
128	25.9	5595.	120.	0.36	0.07	4.23	0.20	5720.	37.	0.16	0.03	4.62	0.16
135	27.4	6019.	82.	0.43	0.10	4.54	0.10	6020.	124.	0.28	0.04	4.38	0.16
139	20.4	5952.	44.	0.28	0.04	4.38	0.10	5880.	116.	0.32	0.04	4.44	0.12
148	35.4	5190.	44.	0.17	0.04	4.40	0.10	5320.	49.	0.02	0.03	4.56	0.12
153	22.1	4725.	44.	0.05	0.04	4.50	0.20	4780.	97.	-0.05	0.09	4.56	0.19

Table 2—Continued

KOI	S/N 5650Å	$T_{\rm eff}$ SME	σ SME	[Fe/H] SME	σ SME	log g SME	σ SME	$T_{\rm eff}$ *Kea*	σ *Kea*	[Fe/H] *Kea*	σ *Kea*	log g *Kea*	σ *Kea*
180	19.0	5680.	60.	0.00	0.06	4.66	0.10	5580.	111.	0.20	0.04	4.50	0.14
180	34.1	5680.	60.	0.00	0.06	4.66	0.10	5740.	68.	-0.06	0.02	4.50	0.10
244	36.8	6103.	47.	-0.10	0.04	4.02	0.10	6300.	84.	-0.07	0.03	4.38	0.07
244	39.6	6103.	47.	-0.10	0.04	4.02	0.10	6320.	73.	-0.10	0.02	4.12	0.07
261	37.5	5692.	44.	0.04	0.04	4.40	0.10	5800.	32.	-0.04	0.03	4.56	0.06
265	32.7	6056.	44.	0.18	0.04	4.29	0.06	6060.	68.	0.14	0.03	4.19	0.12
265	33.7	6056.	44.	0.18	0.04	4.29	0.06	6180.	37.	0.14	0.03	4.56	0.19
273	39.3	5664.	44.	0.24	0.04	4.30	0.06	5780.	49.	0.21	0.03	4.31	0.12
372	21.8	5872.	44.	0.02	0.04	4.64	0.06	5840.	93.	0.03	0.04	4.69	0.06
377	18.8	5777.	61.	0.12	0.04	4.49	0.09	5680.	73.	0.25	0.06	4.19	0.26
377	23.2	5777.	61.	0.12	0.04	4.49	0.09	5800.	32.	0.11	0.03	4.38	0.16
555	19.9	5245.	44.	0.03	0.04	4.37	0.06	5420.	58.	0.03	0.04	4.56	0.19
701	22.8	4925.	70.	-0.37	0.04	4.68	0.07	5020.	58.	-0.56	0.04	4.50	0.10
701	23.1	4925.	70.	-0.37	0.04	4.68	0.07	4960.	60.	-0.45	0.04	4.56	0.12
711	19.2	5502.	44.	0.37	0.04	4.39	0.06	5680.	107.	0.27	0.05	4.06	0.26